Journal of Medicinal Chemistry

Article

High-Affinity Epidermal Growth Factor Receptor (EGFR) Irreversible Inhibitors with Diminished Chemical Reactivities as Positron Emission Tomography (PET)-Imaging Agent Candidates of EGFR Overexpressing Tumors

Eyal Mishani, Galith Abourbeh, Orit Jacobson, Samar Dissoki, Revital Ben Daniel, Yulia Rozen, Mazal Shaul, and Alexander Levitzki

J. Med. Chem., **2005**, 48 (16), 5337-5348• DOI: 10.1021/jm0580196 • Publication Date (Web): 12 July 2005

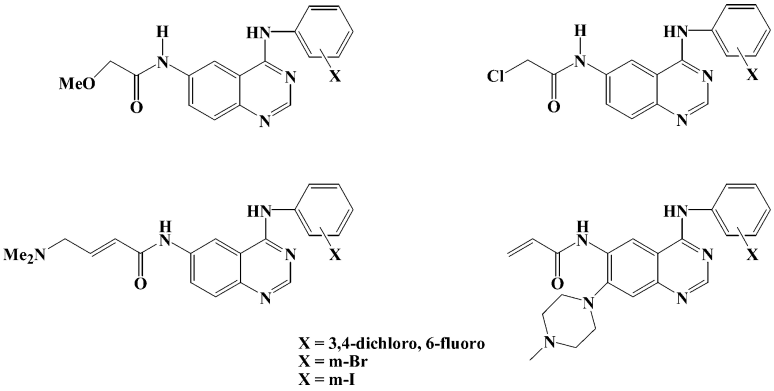

More About This Article

Additional resources and features associated with this article are available within the HTML version:

- Supporting Information
- Links to the 8 articles that cite this article, as of the time of this article download
- Access to high resolution figures
- Links to articles and content related to this article
- Copyright permission to reproduce figures and/or text from this article

View the Full Text HTML

Journal of Medicinal Chemistry is published by the American Chemical Society. 1155 Sixteenth Street N.W., Washington, DC 20036

High-Affinity Epidermal Growth Factor Receptor (EGFR) Irreversible Inhibitors with Diminished Chemical Reactivities as Positron Emission Tomography (PET)-Imaging Agent Candidates of EGFR Overexpressing Tumors

Eyal Mishani,*[,†,‡] Galith Abourbeh,[†,§,‡] Orit Jacobson,[†] Samar Dissoki,[†] Revital Ben Daniel,[†] Yulia Rozen,[†] Mazal Shaul,[†] and Alexander Levitzki[§]

Department of Medical Biophysics and Nuclear Medicine, Hadassah Hebrew University, Jerusalem 91120, Israel, and Unit of Cellular Signaling, Department of Biological Chemistry, The Alexander Silberman Institute of Life Sciences, The Hebrew University, Jerusalem 91904, Israel

Received March 29, 2005

Previous studies with the anilinoquinazoline epidermal growth factor receptor (EGFR) irreversible inhibitor [^{11}C]-ML03 demonstrated a rapid metabolism of the tracer, which led to its low in vivo accumulation in EGFR overexpressing tumors. To enhance tumor uptake, the chemical structure of the compound was modified, and four new groups of EGFR inhibitors with a wide range of chemical reactivities were synthesized. Chemical reactivity assay of the compounds, performed with reduced glutathione (GSH), revealed that the group C (4-(dimethylamino)-but-2-enoic amide) derivative was the least chemically reactive against the nucleophilic attack of GSH. Nonetheless, it demonstrated a high inhibitory potency and bound irreversibly to the EGFR. Consequently, the blood stability of the group C compound (**5a**, ML04) labeled with ^{11}C was studied. In a time frame of 60 min, no radioactive metabolites were detected in blood. The stability of [^{11}C]-**5a**, as indicated both from in vitro blood-stability assays and injection into nude rats, was significantly higher as compared to [^{11}C]-ML03. Since group C presented a greater promise for tumor accumulation, it represents, to date, the most suitable candidate for radiolabeling with long-lived positron emission tomography (PET) radioisotopes.

Introduction

Growth factors, differentiation factors, and hormones are crucial components of the regulatory network that coordinates the development of multicellular organisms. Many of these growth factors mediate their pleiotropic actions through cell surface receptors with an intrinsic protein tyrosine kinase activity. The epidermal growth factor receptor (EGFR/Her-1/ErbB-1), which belongs to the ErbB receptor family, is involved in the proliferation and differentiation of both normal and malignant cells.

The activation of the receptor occurs by a three-step mechanism: (a) binding of specific ligands such as epidermal growth factor (EGF), transforming growth factor α (TGFα), amphiregulin (AR), betacellulin (BTC), epiregulin, or HB-EGF to the receptor at the extracellular ligand-binding domain; (b) dimerization of the ligand−receptor complexes; (c) autophosphorylation of the receptor at the intracellular tyrosine kinase domain. The autophosphorylation serves as a trigger for several downstream signal transduction pathways.[1−5] Following the autophosphorylation, the receptor clusters in coated pits and is endocytosed in vesicles that ultimately either recycle back to the membrane or fuse with lysosomes, where the receptor is degraded.[6]

Overexpression of the EGFR and its enhanced signaling are a frequent hallmark of human epithelial cancers, and it contributes to the initiation, progression, and invasiveness of human cancers.[5,7−9] Thus, the EGFR is an attractive target for the design and development of compounds that can specifically bind the receptor and inhibit its tyrosine kinase (TK) activity and its signal transduction pathway in cancer cells. Such compounds can serve for therapeutics and, when labeled, as targeted diagnostic agents. The EGFR reversible inhibitor gefitinib (ZD1839, Iressa; AstraZeneca, London, United Kingdom) (Figure 1) was approved by the FDA as a third-line treatment of chemotherapy-refractory non-small-cell lung carcinomas (NSCLC).[10] The anti-EGFR antibody Erbitux (cetuximab, ImClone systems, Inc.) has recently gained an accelerated FDA approval as well for the treatment of metastatic, advanced colorectal cancer.[11] Several other anti-EGFR targeted molecules, such as erlotinib (OSI-774, Tarceva; Genentech, San Francisco, CA) (Figure 1), are presently undergoing phase 3 clinical trials. Consequently, there has been a considerable interest in the use of radioactively labeled EGFR inhibitors as bioprobes for positron emission tomography (PET) molecular imaging of EGFR overexpressing tumors.[12−17] PET is a nuclear imaging modality that allows four-dimensional, quantitative determination of the distribution of radioactive probes within the human body. It is used for the measurement of physiological, biochemical, and pharmacological functions at the molecular level, both in normal and in pathological states. PET allows accurate measurements of radioactivity concentrations in small volume compartments in vivo, thus enabling kinetic surveillance of radioactivity throughout the body. PET imaging requires the admin-

* To whom correspondence should be addressed. Fax: 972 2 6421203. Tel: 972 2 6777931. E-mail: mishani@md.huji.ac.il.
† Hadassah Hebrew University.
‡ These authors equally contributed to the article.
§ The Hebrew University.

10.1021/jm0580196 CCC: $30.25
Published on Web 07/12/2005

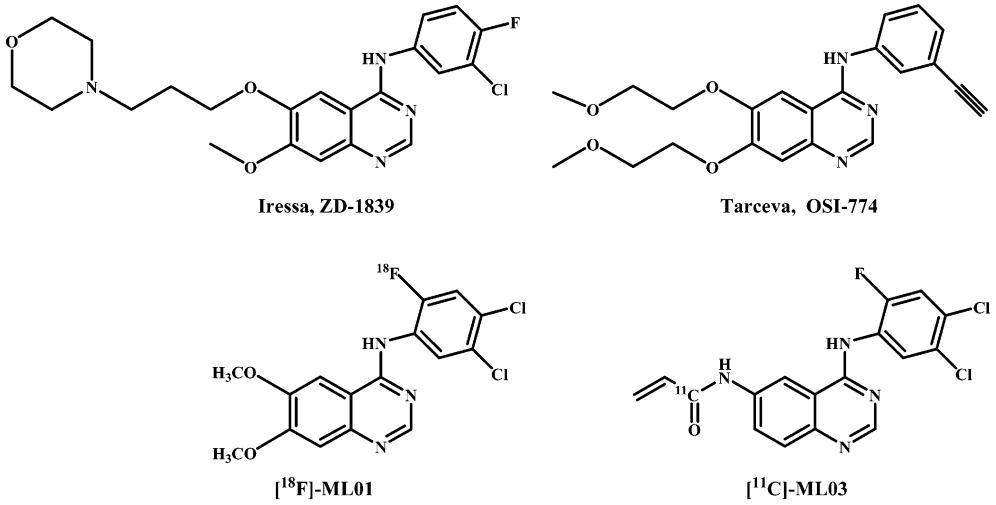

Figure 1. Chemical structures of reversible and irreversible EGFR inhibitors.

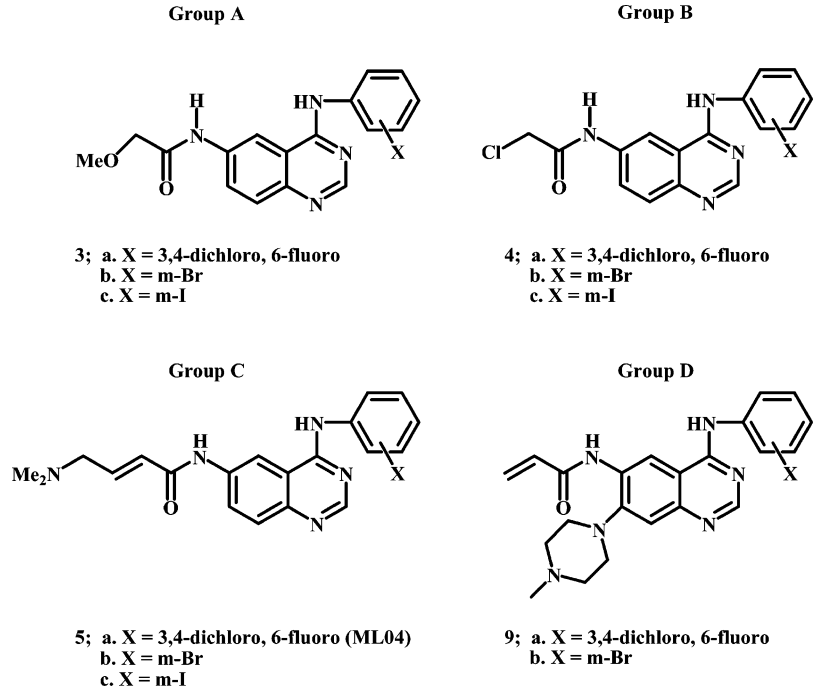

Figure 2. Chemical structures of group A−D inhibitors of the EGFR.

istration of a suitable molecule labeled with a positron emitting nuclide, such as oxygen-15, nitrogen-13, carbon-11, and fluorine-18, which have half-lives of 2.037, 9.965, 20.39, and 109.8 min, respectively.

Biological evaluation of labeled anilinoquinazolines as potential PET−EGFR bioprobes in cancer was previously reported.[18,19] During the course of that study, the uptake of a labeled reversible inhibitor (MLO1) was compared with that of a labeled irreversible inhibitor (MLO3) (Figure 1) in EGFR overexpressing tumors.[18−20] Rapid washout of the labeled reversible inhibitor from the tumor was observed, most likely due to its futile competition with the high intracellular concentration of ATP at the ATP-binding pocket of the receptor.[18] This rapid washout was overcome using the irreversible inhibitor, [^{11}C]-ML03, which covalently binds the EGFR through the acrylamide substituent on the quinazoline ring. Nevertheless, the unsaturated, chemically reactive acrylamide bond of the compound led to its rapid in vivo metabolism, resulting in only a minor accumulation of the labeled compound in the tumor.[19] To decrease the chemical reactivity of the double bond in the acrylamide moiety and enhance tumor availability, modifications of the functional group at the 6-position of the quinazoline ring were made. We report here on the syntheses of new EGFR inhibitors (Figure 2), their relative chemical reactivities, and their inhibitory potencies.

Results

Chemistry. The syntheses of compounds **3**−**5** and **9** are outlined in Scheme 1. 6-Nitroquinazolone was reacted with thionyl chloride to produce the 4-chloro-6-nitroquinazoline. The excess of thionyl chloride was distilled out, and the product was obtained without any further purification, with 80% chemical yield and 97% purity, as determined by HPLC. Reaction of the 4-chloro-6-nitroquinazoline was performed with either of the following aniline derivatives: 3,4-dichloro-6-fluoroaniline (**a**), *meta*-bromoaniline (**b**) or *meta*-iodoaniline (**c**) in *i*-PrOH at reflux. The products were obtained as

Scheme 1. Chemical Syntheses of Group A–D Inhibitors of EGFR

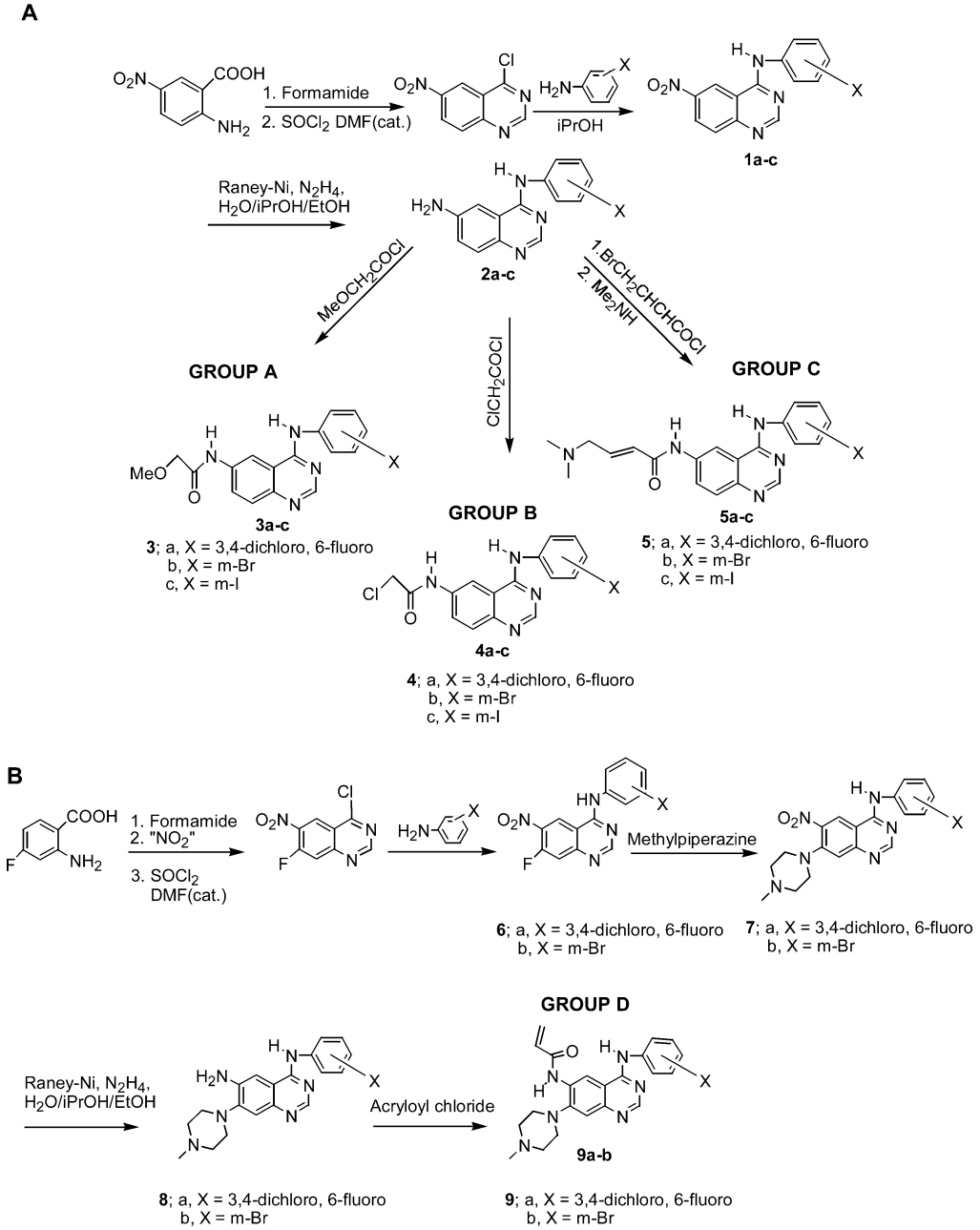

a bright yellow precipitate. After filtration, compounds **1a**–**c** were obtained with 75%–80% yield. In the next step, the nitro group at the 6-position of the quinazoline ring was reduced to amine. It should be noted that an undesired reduction of the halogen position at the anilino moiety was observed only with the iodo derivative. Therefore, the reduction step of this derivative was performed at 0 °C. Yet, even at this temperature, we observed 10% formation of the reduction side product that was separated from the desired product by silica chromatography. Compounds **2a**–**c** were used as basic starting materials for the preparation of the three different groups of inhibitors. They were reacted with α-methoxyacetyl chloride to yield group A compounds, **3a**–**c**, with 71%, 69%, and 64% yield, respectively. Reaction with α-chloroacetyl chloride yielded group B compounds, **4a**–**c**, with 74%, 40%, and 27% yield, respectively. Group C compounds, **5a**–**c,** were obtained after a two-step synthesis, as described in Scheme 1, with 20% yield. The synthesis of group D was started with reaction of fluoroantrinilic acid and formamide to obtain the quinazoline (Scheme 1B). Nitration and then chlorination with thionyl chloride yielded the nitrochloroquinazoline. Coupling with the appropriate anilino derivative and reaction with methylpiperazine, followed by reduction of the nitro group and reaction with acryloyl chloride provided group D compounds, **9a**,**b**, with an overall average yield of 11%.

Radiochemistry. Carbon-11-labeled MeI was prepared according to a well-documented procedure and reacted with 8 mg of 4-monomethyl-amino-but-2-enoic acid [4-(3,4-dichloro-6-fluoro-phenylamino)-quinazolin-6-yl]-amide precursor.[14] The product, [^{11}C]-**5a**, was obtained after a 50 min total radiosynthesis time, including HPLC purification, with an average ($n = 30$) final dose of approximately 0.74 GBq (20 mCi, 10% decay-corrected radiochemical yield) and a specific activity of 2.1–3.3 Ci/μmol.

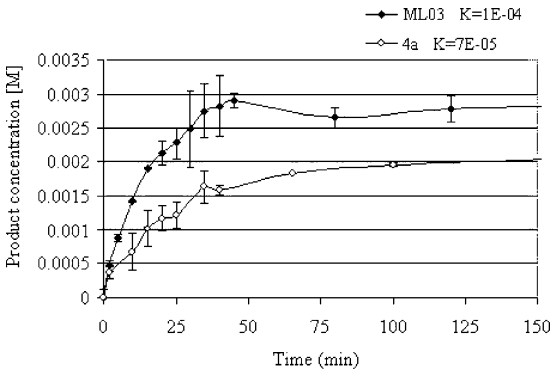

Figure 3. Reaction profiles of compounds **4a** and ML03 with reduced glutathione. Compounds were dissolved in THF−MeOH−H_2O (1:2:1) and reacted at room temperature with $^1/_2$ equiv of reduced glutathione in the presence of *N*,*N*′-diisopropylethylamine. The conversion rate into GSH conjugates was measured as described in the text.

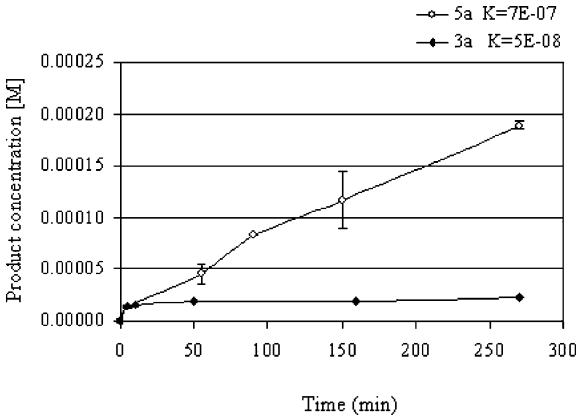

Figure 4. Reaction profiles of compounds **3a** and **5a** with reduced glutathione. Compounds were dissolved in THF−MeOH−H_2O (1:2:1) and reacted at room temperature with $^1/_2$ equiv of reduced glutathione in the presence of *N*,*N*′-diisopropylethylamine. The conversion rate into GSH conjugates was measured as described in the text.

Challenge Reaction with Reduced Glutathione. EGFR blockade by irreversible inhibitors is due to the nucleophilic attack of the sulfhydryl group of Cys-773 at the ATP binding pocket of the receptor on the reactive chemical group of the EGFR-targeted inhibitor.[21] To mimic this reaction, we examined the degree of reactivity of the inhibitors toward the sulfhydryl group of reduced glutathione (GSH). Compounds **3**−**5a** and ML03 were dissolved in THF/MeOH/H_2O (1:2:1) and reacted at room temperature with $^1/_2$ equiv of reduced glutathione in the presence of 12 equiv of *N*,*N*-diisopropylethylamine. Identical aliquots of the reaction mixtures were taken at various time points and injected into reversed-phase HPLC to determine the conversion rate of the various compounds into glutathione conjugates. The characteristics of the products were determined using MS. For each of the four reactions, a graph of product concentration as a function of time was plotted (Figures 3 and 4). Reaction rate constants of 5×10^{-8}, 7.0×10^{-5}, 7.0×10^{-7}, and 1.0×10^{-4} M/min were measured for compounds **3**−**5a** and ML03, respectively. In a study of the reaction rate as a function of the temperature (Figures 5 and 6), activation parameters were obtained as follows: for ML03, $E_a = 5.24$ kcal mol^{-1}, $\Delta H^{\ddagger}_{25°C} = 4.64$ kcal mol^{-1}, and $\Delta S^{\ddagger}_{25°C} = -61.24$ cal mol^{-1} K^{-1}; for compound **4a**, $E_a = 11.4$ kcal mol^{-1}, $\Delta H^{\ddagger}_{25°C} = 10.80$ kcal mol^{-1}, and $\Delta S^{\ddagger}_{25°C} = -41.29$ cal mol^{-1} K^{-1}. Activation energies of compounds **3a** and **5a** were too high; thus even at temperatures exceeding 100 °C, we could not obtain a change in the reaction rate.

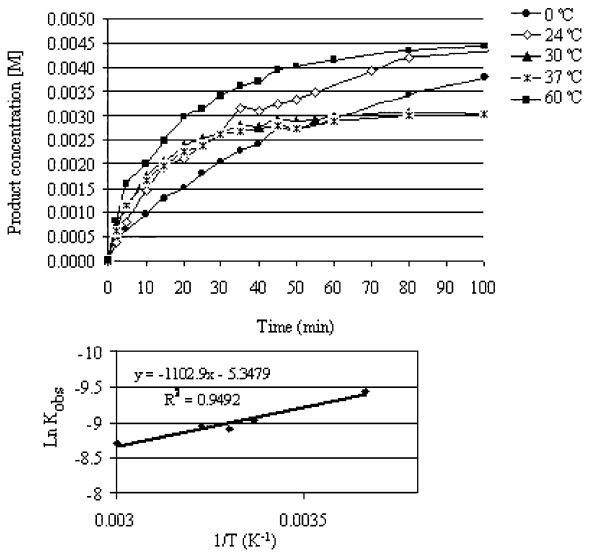

Figure 5. Calculation of activation energy of ML03: $E_a = 5.24$ kcal mol^{-1}, $\Delta H^{\ddagger}_{25°C} = 4.64$ kcal mol^{-1}, and $\Delta S^{\ddagger}_{25°C} = -61.24$ cal mol^{-1} K^{-1}.

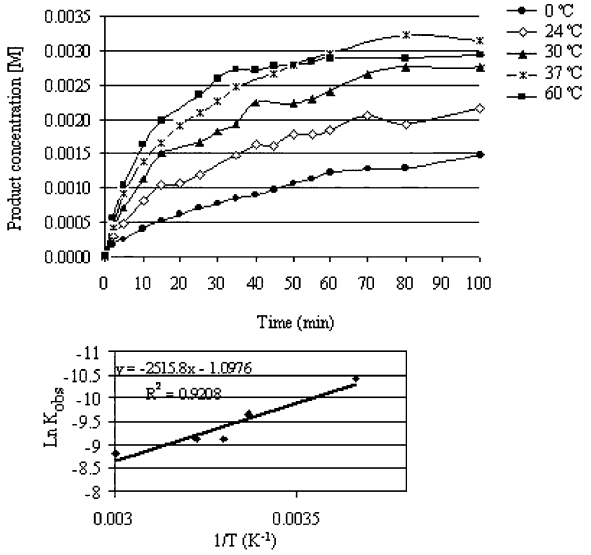

Figure 6. Calculation of activation energy of compound **4a**: $E_a = 11.4$ kcal mol^{-1}, $\Delta H^{\ddagger}_{25°C} = 10.80$ kcal mol^{-1}, and $\Delta S^{\ddagger}_{25°C} = -41.29$ cal mol^{-1} K^{-1}.

The results of the challenge assay of the different groups of compounds with reduced glutathione placed groups A and C as the most chemically stable compounds regarding the nucleophilic attack performed by the sulfhydryl group of GSH.

Biology. IC_{50} Evaluation Assays. Two different methods were used to measure EGFR-TK autophosphorylation IC_{50} values of the inhibitors and the reference inhibitor, ML03. In the first method, the inhibitors were evaluated in a cell-free system by means of ELISA to determine their EGFR autophosphorylation IC_{50} values. The assays were performed with A431 cell lysates (human epidermoid vulval carcinoma cells), which overexpress the EGFR. The apparent IC_{50} averages of each

Table 1. IC_{50} Values in the ELISA Screen and in Intact A431 Cells[a]

			Intact A431 cells	
		A431 lysate		
group	structure	IC_{50} app[b] [nM]	IC_{50} range[c] (immediately after removal of the inhibitor) [nM]	IC_{50} range[c] (8 h after removal of the inhibitor) [nM]
	ML01	0.208	3−5	
	ML03	0.037	6.7−20	6.7−20
group A	**3a**	252 ± 137	1000−10000	10000−50000
	3b	174 ± 135	>13000	>100000
	3c	150 ± 135	1000−5000	∼50000
group B	**4a**	0.07 ± 0.03	5−25	25−50
	4b	0.4−32	<5	∼10
	4c	0.11−0.12	4−10	∼30
group C	**5a**	0.11 ± 0.08	4−10	10−50
	5b	0.41 ± 0.39	1−10	1−10
	5c	0.94 ± 0.90	<5	<5
group D	**9a**	6000 ± 5000	∼250	>500
	9b	500−13000	50−250	>500

[a] The ELISA was performed with A431 cell membranes. IC_{50} values in intact A431 cells refer to inhibition of EGFR phosphorylation immediately after and 8 h after removal of the compound from the medium. [b] The IC_{50} values for each derivative were obtained from three independent experiments, at least, and are represented as either mean ± standard deviation or as a range. [c] For each compound, at least two different assays with similar results were performed. Each experiment was performed in duplicate.

compound were obtained from three independent dose response curves and are summarized in Table 1. Unlike the results that were obtained in the GSH assay, the results of these experiments revealed that group B and C compounds possessed the highest inhibitory potencies toward the EGFR and were on a par with ML03. Their average IC_{50} values were in the sub-nanomolar range, whereas those of group A and D compounds were about 2−3 orders of magnitude higher.

To assess the irreversible inhibitory effect of the compounds upon EGFR autophosphorylation, in the second method, each inhibitor was incubated with intact A431 cells for 1 h, as described in the Experimental Section, and the degree of EGFR phosphorylation was measured either immediately after or 8 h after removal of the inhibitor from the medium. The results presented in Figure 7 are summarized in Table 1. In accordance with the data that were obtained from the cell-free assays, the studies with intact A431 cells demonstrate that not only were group B and C compounds more potent than their analogues of groups A and D in inhibiting the EGFR but the former also retained their inhibitory effect on receptor phosphorylation even 8 h after their removal from the medium, affirming that these inhibitors are covalently bound to the receptor.

Blood Stability of [^{11}C]-ML03 and [^{11}C]-5a and in Vivo Metabolism Assessment. It was previously demonstrated that following incubation of [^{11}C]-ML03 with blood samples, the total extracted radioactivity decreased from 65% to 50% within 1 h with no apparent formation of radioactive metabolites.[19] To compare the blood stability of ML03 with that of compound **5a**, a similar assay was performed with the latter. Briefly, [^{11}C]-**5a** was incubated with blood samples at 37 °C for different time periods. Blood samples were extracted with ethanol/THF (1:1), the extracted radioactivity was loaded on reversed-phase TLC plates, and radioactive bands were visualized by a phosphor imager plate. The average total basal extracted radioactivity by this method was 61%, all of which corresponded to [^{11}C]-**5a**.

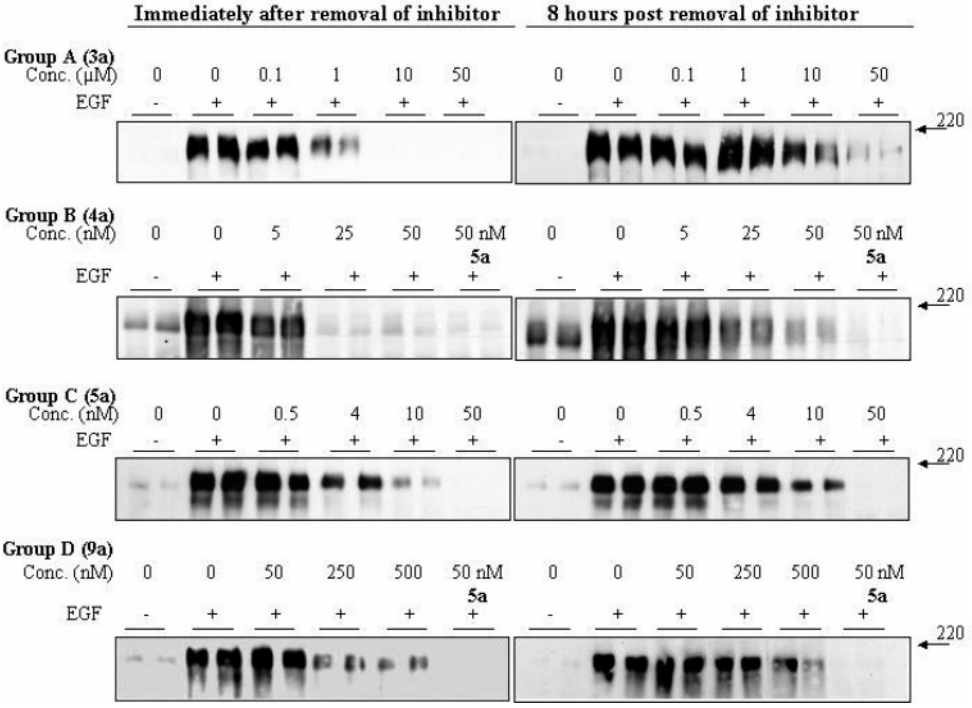

Figure 7. Extent of irreversible inhibitory effect of group A−D compounds upon EGFR phosphorylation, as indicated by its anti-phosphotyrosine (αPY) content. A431 cells were incubated with the investigated compound for 1 h and stimulated with EGF (20 ng/mL) either immediately after or 8 h after removal of the compound from the medium. Cell lysates (10 μg of total protein) were loaded onto 8% SDS−PAGE, and EGFR anti-phosphotyrosine content was measured. Blots of one demonstrative compound (**a** derivative) from each group (A−D) are presented.

Table 2. IC_{50} Values of Group A−C Compounds (**a** Derivative) for Inhibition of Phosphorylation of HER1, HER2, and PDGFR Kinase Domains in Intact DHER14, CSH12, and NIH/PDGFR Cells, Respectively

	IC_{50} value (nM)		
structure	DHER14	CSH12	NIHPDGFR
3a	>250	>500	>1000
4a	5−15	25−50	>1000
5a	~4	25−50	>1000

Within 60 min of incubation, the total extracted radioactivity remained identical (data not presented). As with [^{11}C]-ML03, formation of radioactive metabolites was not detected within 1 h of measurement by this extraction method. However, while the total extracted radioactivity of [^{11}C]-ML03 samples decreased by nearly 25% within 1 h, it remained unchanged with [^{11}C]-**5a**. Most likely the nonextractable fractions could be accounted for by binding to sulfhydryl groups of plasma proteins. These results are in good agreement with those obtained in the GSH assay and reflect the superior chemical stability of compound **5a** over ML03.

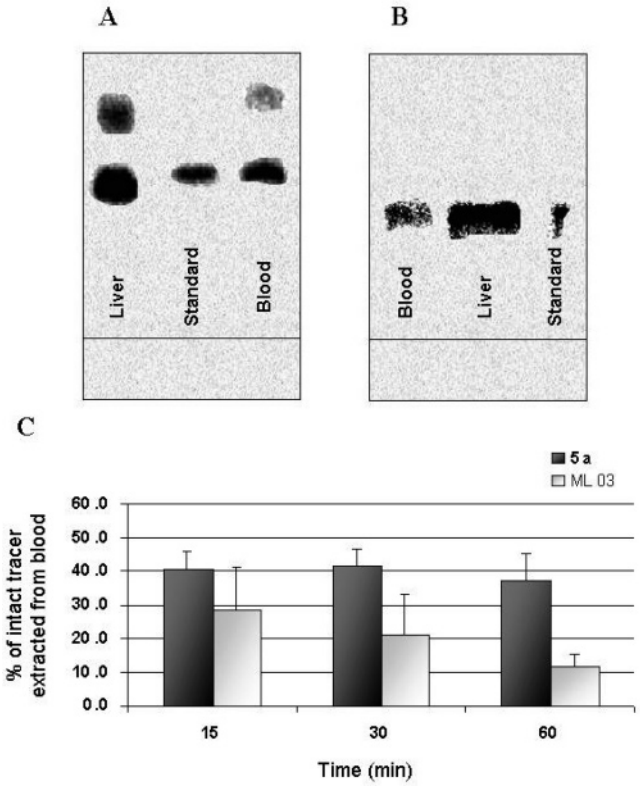

Figure 8. In vivo stability of [^{11}C]-ML03 compared to [^{11}C]-**5a**. Nude Hsd:RH-rnu/rnu rats were injected with about 250 μCi of either [^{11}C]-ML03 or [^{11}C]-**5a** and sacrificed at predetermined time points. The total extracted radioactivity from the blood and the liver was measured and loaded onto RP TLC plates next to a standard for detection of radioactive metabolites. Panel A shows extracted radioactivity from blood (right panel) and liver (left panel), as compared to the standard (middle) 30 min postinjection of [^{11}C]-ML03. Panel B shows extracted radioactivity from blood (left panel) and liver (middle panel), as compared to the standard (right) 60 min postinjection of [^{11}C]-**5a**. Panel C shows a quantitative comparison of intact tracer extracted from blood following injection of the labeled tracer into nude rats. For each labeled compound, the percent extraction of intact tracer was calculated by multiplying the total extracted radioactivity from 1.5 mL blood by the TLC fraction of the radioactive band, corresponding to the tracer, as previously described.[19]

For further establishment of relative reactivities of [^{11}C]-ML03 versus [^{11}C]-**5a**, an in vivo evaluation of stability was performed. Briefly, around 250 μCi of the C-11-labeled compounds were injected into rats; at predetermined time points, the rats were sacrificed, blood was drawn, livers were excised, and the extracted radioactivity was loaded onto reversed-phase TLC plates. The radio-chromatograms of the extracted radioactivity, which are presented in Figure 8A,B, revealed that while metabolite formation was observed at a rather early stage with [^{11}C]-ML03, no metabolite formation was detected for the C-11-labeled compound **5a** 60 min postinjection. Altogether, the improved chemical stability of compound **5a**, as compared to ML03, along with its potent irreversible inhibitory effect of the EGFR, set it as a more promising candidate for in vivo imaging of EGFR overexpressing tumors.

Selectivity Assays. Binding selectivity of a PET probe to its molecular target is a significant determinant of its ability to serve as a high-quality imaging agent. To characterize the degree of specificity of the compounds in inhibiting the EGFR, one representative compound (the **a** derivative) of groups A−C was tested out in a cellular assay, similar to the assay performed with A431 cells. Group D compounds were excluded from this assay due to their less favorable profile, namely, high chemical reactivity and poorer inhibitory potency. In brief, DHER14, CSH12, and NIH/PDGFR cells expressing EGFR, EGFR−human epidermal growth factor receptor 2 (HER2) chimera, or platelet-derived growth factor receptor (PDGFR), respectively, were incubated with the tested inhibitor for 1 h.[22−24] Following removal of the inhibitor from the medium and stimulation with the appropriate growth factor, the cells were harvested, and the extent of inhibition was evaluated by measuring the phosphotyrosine content of the receptor in a Western blot analysis. The data presented in Table 2 reveal that all three groups of compounds bear no inhibitory effect upon the PDGFR (IC_{50} > 1 μM). Nonetheless, the inhibitory profile with respect to the kinase domain of HER2 and EGFR was similar to that observed in A431cells: groups B and C were far more potent in inhibiting both EGFR/c-ErbB1 (IC_{50} = 4−15 nM) and c-ErbB2 (IC_{50} = 25−50 nM) than group A (IC_{50} > 0.5 μM). These results indicate that group B and C inhibitors possess higher affinities toward the c-ErbB family of receptors than toward the PDGFR.

Discussion

In previous studies with the labeled irreversible inhibitor [^{11}C]-ML03, high metabolic rate and low tumor availability were observed, resulting in a moderate tumor to blood uptake ratio of the tracer.[19] Thus, to enhance tumor uptake and improve the quality of images, our aim was to explore new chemically modified EGFR irreversible inhibitors, which hold higher stability and less reactivity. With this in mind, four new groups of EGFR inhibitors with varying extents of chemical reactivities toward nucleophilic attack were synthesized as candidates for radiolabeling with PET isotopes. The same basic structure as the acrylamidoquinazoline derivative, ML03, was used with strategic changes that were intended to reduce the chemical

reactivity of the double bond of the acrylamide moiety toward nucleophilic attacks. It is highly probable that interactions of this kind between blood and plasma components and the inhibitors exist, hampering the tumor availability of the labeled compound. The chemical modifications were performed at the 6-position of the quinazoline ring (Figure 2). The highly chemically reactive acrylamide group at the 6-position of ML03 was replaced with either α-methoxyacetamide (group A), α-chloroacetamide (group B), or 4-dimethylaminocrotonylamide (group C) (the last group was first introduced by Tsou et al.[25]) In these groups, the α carbon (groups A and B) or the β carbon (group C) is partially positively charged and thus sufficiently reactive toward the nucleophilic attack by Cys-773 at the EGFR kinase domain. Moreover, it is likely that Cys-773 is ionized to the S^- form, enabling efficient interaction with less reactive electrophiles, such as group A−C inhibitors. The higher energy gap of the HOMO−LUMO electronic orbitals of the reactive carbon centers of these compounds, as compared to that of the β carbon in the acryloyl group of ML03, increases their chemical stability, thereby augmenting the biological stability of the compounds and, hopefully, their tumor availability. Thus, if the inhibitory potencies were not dramatically affected and remained at the nanomolar range, the new inhibitors would remain at the receptor binding site long enough to allow covalent bonding. By retaining the double bond of the acrylamide intact (group D compounds), we aimed at preserving the chemical reactivity toward nucleophilic attack. Instead, we wished to modify the solubility of the molecule by adding the methylpiperazine group at the 7-position of the quinazoline ring. As previously mentioned, each group contained elements that could enable radiolabeling with C-11, F-18, iodine, or bromine PET isotopes. The substantially longer half-life of I-124 and Br-76 may offer prolonged monitoring following injection of the radiotracer. Such monitoring could be possible, providing that the labeled tracer stays long enough in the environment of the receptor. The acrylamide moiety at the 6-position of the quinazoline ring is known to confer to this type of inhibitor a covalent, irreversible binding nature to the EGFR.[21] These data were supported by performing assays with intact A431 cells in which the long-lasting inhibitory effect of the compounds was evident even 8 h after removal of the inhibitors and successive rinse of the media. The stable interaction between the receptor and the labeled inhibitor guarantees that the tracer is not eliminated from the tumor cells, thus leaving adequate time for imaging.

To prepare the new groups of irreversible EGFR inhibitors, the chemical route described by Tsou et al.[25] and Fry et al.[21] was followed with minor modifications (Scheme 1). The synthesis of groups A−C started with nitroantranilic acid, and a reaction with formamide, followed by chlorination, yielded the 4-chloro-6-nitroquinazoline. Coupling with the appropriate anilino derivative, followed by reduction of the nitro group, provided the basic anilinoquinazoline derivative from which each group was obtained. Reactions with methoxyacetyl chloride, chloroacetyl chloride, and bromocrotonyl chloride (followed by reaction with dimethylamine) yielded groups A, B, and C, respectively. Group D compounds were obtained by the chemical route described in Scheme 1B, starting with fluoroantranylic acid, with an overall yield of 11%.

To evaluate the chemical reactivity of the formerly studied compound, ML03, as well as of the new groups of compounds (groups A−C), we reacted one derivative from each group (dichlorofluoroaniline derivative) with the sulfhydryl-containing tripeptide glutathione as nucleophile and measured the reaction rate constants (Figures 3 and 4). As was anticipated, ML03 was found to be the most chemically reactive compound toward the nucleophilic attack performed by the sulfhydryl group of GSH, and the addition reaction went on with a reaction rate constant of 1.0×10^{-4} M/min. The chloroacetamide derivative of group B was found to be less reactive, possessing a reaction rate constant of 7.0×10^{-5} M/min. Group A and C derivatives were found to be far more stable toward the nucleophilic attack of the sulfhydryl group, possessing reaction rate constants of 5.0×10^{-8} and 7.0×10^{-7} M/min, respectively. Moreover, by determination of the reaction rate as a function of temperature (Figures 5 and 6), the activation energies measured for ML03 and compound **4a** were 5.24 and 11.4 kcal mol^{-1}, respectively. The considerably higher activation energies of compounds **3a** and **5a**, relative to the group B derivative and ML03, prevented us from measuring any change in the reaction rate even at temperatures exceeding 100 °C. On the whole, these results suggest that group A and C compounds are more chemically stable as compared to ML03 and group B compounds.

Since the actual interaction between the inhibitor and the receptor is comprised of several components and is not merely based on a nucleophilic attack,[21] the new irreversible inhibitors were evaluated in vitro by means of ELISA to determine their EGFR autophosphorylation IC_{50} values (Table 1). According to this assay, group B and C compounds, along with ML03, were the most potent EGFR inhibitors out of the four investigated groups. The IC_{50} values of groups B and C, in the subnanomolar range, were 2−3 orders of magnitude lower than those of groups A and D. On the whole, the more chemically reactive compounds, **4a** and ML03, were also more potent in inhibiting the receptor, whereas the more chemically stable compound, **3a**, exhibited the lowest inhibitory potency. Nonetheless, the relatively chemically stable compound, **5a**, according to the GSH assay was among the most potent inhibitors of the EGFR as well. To affirm this favorable in vitro profile of minimal reactivity toward sulfhydryl groups combined with high EGFR affinity, the extent of inhibition in terms of reversibility and potency was further investigated in a cellular assay. It should be noted that the ELISA screen provided adequate information regarding the relative inhibitory potencies of the different groups; nevertheless, this assay was not sensitive enough to differentiate between the derivatives in each group. The lack of highly reproducible differences in IC_{50} values within each group prevented us from favoring one particular substituent. An evaluation of the irreversible inhibitory effect of the compounds was provided by incubating each inhibitor with intact A431 cells for 1 h and measuring the degree of EGFR phosphorylation either immediately after or 8 h after removal of the inhibitor from the medium. As previously described,[26] an inhibitor could

be considered as an irreversible one if 80% inhibition or more is achieved 8 h after its removal from the medium, whereas 20−80% inhibition classifies the compound as "partially irreversible." According to this standard, the data in Table 1 indicate that group A compounds were reversible (80% inhibition after 8 h was achieved only at concentrations above 10 μM), whereas group B and C compounds exhibited an irreversible inhibitory effect upon the EGFR at 200-fold lower concentrations. Group D compounds, albeit irreversible, were less potent than the prototype compound, ML03. These results further support the superior inhibitory potency of group B and C compounds over group A and D compounds with regard to the EGFR, despite the relatively chemically stable nature (as indicated by the GSH assay) of compound **5a**, a demonstrative inhibitor of group C compounds. The irreversible inhibitory effect of group B compounds presumably results from covalent bonding to the kinase domain of the EGFR. This suggests that a side chain of three atoms attached at the 6-position of the quinazoline moiety, as in group B compounds, is sufficient to attain irreversible binding to the receptor. As a result of these superior chemical and biological qualities of group C compounds in general and of derivative **5a** in particular, ex vivo and in vivo stability assessments of the compound were conducted. For the following radioassays with [^{11}C]-**5a**, the radiolabeling approach was based on C-11 methylation reaction of the monomethylamine group of the amide attached to the 6-position of the quinazoline ring, using C-11 methyl iodide as the labeling agent.[27] The total synthesis time was 50 min, and the final average dose was 0.74 GBq (20 mCi, 10% decay-corrected radiochemical yield (n = 30)); specific activity was 2.1−3.3 Ci/μmol. HPLC analysis of the labeled product solution revealed high radiochemical (>99%) and chemical purities.

The stability of [^{11}C]-**5a** in blood was assessed by incubation of the labeled compound with blood samples at 37 °C for different time periods. The extracted radioactivity was calculated by measurements of total and nonextractable radioactivities and was loaded on TLC plates for visualization of radioactive bands by a phosphor imager plate. The results indicated that the basal extraction of total radioactivity by this method was approximately 65%, all of which corresponded to [^{11}C]-**5a**. Within 60 min of incubation, no metabolites were detected on the radio-chromatogram, and the total extracted radioactivity remained the same. In contrast, previous studies with [^{11}C]-ML03 indicated that the percent of extractable [^{11}C]-ML03 from blood samples throughout 60 min of incubation decreased roughly by 25%, thus revealing a more durable stability of [^{11}C]-**5a** in blood.[19]

For in vivo characterization of stability, a similar assay was performed: rats were injected with the tracer, blood was drawn, and their livers were excised and homogenized. As in the blood-stability assay, the total extracted radioactivity was measured and loaded on TLC plates. The results of two assays with the previously studied compound, [^{11}C]-ML03, as well as with [^{11}C]-**5a** are presented in Figure 8 for comparison. Whereas metabolite formation was observed at a rather early stage with [^{11}C]-ML03, no radioactive metabolites were detected 60 min following injection of [^{11}C]-**5a** into rats. In accordance with the in vitro observations, the blood stability of [^{11}C]-**5a** in rats exceeded that of [^{11}C]-ML03 throughout the 1-h experiment. The stability of [^{11}C]-**5a** in comparison to [^{11}C]-ML03, as indicated by the extractable intact tracer from blood 15 min postinjection into nude rats, was approximately 50% higher. The superior stability profile of this tracer is even further supported given the fact that within 60 min following injection of the tracers, the total extractable intact tracer was 3-fold higher in the case of [^{11}C]-**5a**, as compared to the previously studied labeled EGFR irreversible inhibitor [^{11}C]-ML03 (Figure 8C). Finally, a representative preliminary selectivity examination of group A−C compounds revealed a good selectivity profile of group B and C derivatives, indicated by more than 3-fold higher inhibitory concentrations for the PDGFR vs the erbB-1 and -2 kinase domains.

Conclusion

To enhance the tumor uptake of irreversible EGFR inhibitors and to enable improved future in vivo imaging qualities of labeled EGFR bioprobes, four new groups of EGFR inhibitors with diminished chemical reactivities were synthesized as candidates for PET molecular imaging agents. Enhanced stability characteristics of group C compounds were demonstrated by chemical reactivity assays with reduced GSH, as well as by ex vivo and in vivo blood-stability studies. Altogether with the highly selective and irreversible inhibition profile of this group, these data identify group C compounds as the most suitable candidates for visualization of EGFR overexpressing tumors.

Experimental Section

General. All chemicals were purchased from Sigma-Aldrich, Fisher Scientific, Merck, or J. T. Baker. Chemicals were used as supplied, excluding THF, which was refluxed over sodium and benzophenone and freshly distilled prior to use. Mass spectroscopy was performed in EI mode on a Thermo Quest, Finnigan Trace MS mass spectrometer at the Hadassah-Hebrew University Mass Spectroscopy Facility. ^{1}H NMR spectra were obtained on a Bruker AMX 400 MHz instrument. Elemental analysis was performed at the Hebrew University Microanalysis Laboratory. Radiosyntheses were carried out on a [^{11}C]-CH_3I module (Nuclear-Interface, Munster, Germany). Specific radioactivities were determined by HPLC, using cold mass calibration curves. [^{11}C]-CO_2 was produced by the ^{14}N(p,α)^{11}C nuclear reaction on nitrogen containing 1% oxygen, using an 18/9 IBA-cyclotron. Bombardment was carried out for 15−30 min with a 26 μA beam of 16 MeV protons. At the end of bombardment, the target gas was delivered and trapped by a cryogenic trap in the [^{11}C]-CH_3I module.

Primary antibodies were obtained as follows: PY20 anti-phosphotyrosine (diluted 1:2000) from Santa Cruz Biotechnology Inc. 4G10 anti-phosphotyrosine antibody (1:100 dilution) was produced from Su4G10 hybridoma cells. Horseradish peroxidase-conjugated anti-mouse IgG (1:10000 dilution) was obtained from Jackson Immuno Research Growth factors. Human recombinant EGF and PDGF$_{\beta\beta}$ were purchased from Sigma-Aldrich, Inc.

Cell Culture. NIH3T3 cells transformed with either the EGFR (DHER14 cells), the HER1−HER2 chimera (CSH12 cells), or the PDGFR (NIH/PDGFR cells) have been described.[22−24] These and A431 human epidermoid vulval carcinoma cells were grown in Dulbecco's modified Eagle's medium (DMEM) (Biological industries, Kibbuts Beit Haemek, Israel) supplemented with 10% fetal calf serum and antibiotics (penicillin 10^5 units/L, streptomycin 100 mg/L) at 37 °C in 5% CO_2.

Animal Studies. Nude-Hsd:RH-rnu male rats (11−12 weeks), weighing 250−300 g, were obtained from Harlan Industries, Inc. All animal studies were conducted under a protocol approved by the Research Animal Ethics Committee of the Hebrew University of Jerusalem and in accordance with its guidelines.

Reactions with Reduced Glutathione. Standard solutions were prepared by dissolving compounds **3**−**5a** and ML03 (0.0146 mmol) in 1.75 mL of THF/MeOH (1:2) and glutathione (18 mg (0.0586 mmol)) in 0.5 mL of water. A 300 μL aliquot of the quinazoline standard solution (2.5 μmol) was diluted with 689 μL of THF/MeOH/H_2O (1:2:1), after which 11 μL (1.25 μmol) of glutathione solution and 5.22 μL (30 μmol) of *N*,*N*′-diisopropylethylamine were added. Conversions of the quinazolines and formation of conjugates at different time points were measured by HPLC using RP (3.9 mm × 300 mm) column (mobile phase, acetonitrile and acetate buffer 0.1 M (2:3) at a flow rate of 1 mL/min). The glutathione conjugates were detected by MS as well.

A study of the reaction rate as a function of the temperature generated the following activation parameters: for ML03, E_a = 5.24 kcal mol^{-1}, $\Delta H^{\ddagger}_{25°C}$ = 4.64 kcal mol^{-1}, and $\Delta S^{\ddagger}_{25°C}$ = −61.24 cal mol^{-1} K^{-1}; for compound **4a**, E_a = 11.4 kcal mol^{-1}, $\Delta H^{\ddagger}_{25°C}$ = 10.80 kcal mol^{-1}, and $\Delta S^{\ddagger}_{25°C}$ = −41.29 cal mol^{-1} K^{-1}.

For compounds **3a** and **5a**, the activation energies were too high; thus even at temperatures exceeding 100°C, no change in the reaction rate was obtained.

The rate equation is presented as follows:

$$\frac{-\mathrm{d}[\mathrm{ML0}x]}{\mathrm{d}t} = k_{\mathrm{obs}}[\mathrm{ML0}x][\mathrm{GSH}]$$

$$k_{\mathrm{obs}} = A\ \mathrm{e}^{-E_a/(RT)}$$

where [ML0*x*] and [GSH] represent the concentrations of the tested compound and of glutathione, respectively.

Chemistry. Compounds **1a**−**c**, **2a**−**c** and **5a**−**c** were already prepared (ref 26 and references therein). Compound **6b** was also synthesized.[28]

***N*-{4-[(3,4-Dichloro-6-fluoro-phenyl)amino]-quinazoline-6-yl}-2-methoxyacetamide (3a).** 6-Amino-4-(4,5-dichloro-2-fluoro-phenylamino)-quinazoline (**2a**) (62.4 mg, 0.193 mmol) and triethylamine (53 μL, 39 mg, 0.386 mmol) were dissolved in dry THF (20 mL) and cooled to 0 °C. 4-Methoxyacetyl chloride (35 μL, 42 mg, 0.39 mmol) was added, and the mixture was stirred at 0 °C for half an hour. The mixture was poured into saturated $NaHCO_3$ (30 mL) and extracted with ethyl acetate (3 × 30 mL). The organic solution was dried with Na_2SO_4 and evaporated. The crude material was purified by silica gel chromatography (eluent 4% MeOH in CH_2Cl_2), generating pure **3a** with 71% yield. Mp = 204−206 °C; MS (*m*/*z*) 395.0 (MH$^+$); ^{1}H NMR (DMSO-d_6) δ 10.13 (s, 1H), 9.94 (s, 1H), 8.73 (s, 1H), 8.48 (s, 1H), 7.98 (d, J = 3.3 Hz, 1H), 7.93 (d, J = 3.0 Hz, 1H), 7.9 (d, J = 11.4 Hz, 1H), 7.79 (d, J = 13.8 Hz, 1H), 4.09 (s, 2H), 3.42 (s, 3H). Anal. ($C_{17}H_{13}Cl_2FN_4O_2$) C, H, N. HPLC conditions: C-18 column, 60% acetate buffer, pH = 3.8/40% acetonitrile, flow = 1 mL/min, R_t = 18.39 min.

***N*-{4-[(3-Bromo-phenyl)amino]-quinazoline-6-yl}-2-methoxyacetamide (3b).** This compound was prepared in the same manner as compound **3a**, described above, and was purified by silica gel chromatography (eluent 3% MeOH in CH_2Cl_2) to yield pure **3b** with 69% yield. Mp = 190−191 °C; MS (*m*/*z*) 387.0 (MH$^+$); ^{1}H NMR (DMSO-d_6) δ10.1 (s, 1H), 9.9 (s, 1H), 8.72 (d, J = 3.6 Hz, 1H), 8.6 (s, 1H), 8.2 (t, J = 3.6 Hz, 1H), 8.01 (dd, J_1 = 16 Hz, J_2 = 3.6 Hz, 1H), 7.87 (dt, J_1 = 13 Hz, J_2 = 3.4, 1H), 7.82 (d, J = 16 Hz, 1H), 7.3 (m, 2H), 4.1 (s, 2H), 3.4 (s, 3H). Anal. ($C_{17}H_{15}BrN_4O_2$) C, H, N. HPLC conditions: C-18 column, 60% acetate buffer, pH = 3.8/40% acetonitrile, flow = 1 mL/min, R_t = 13.4 min.

***N*-{4-[(3-Iodophenyl)amino]-quinazoline-6-yl}-2-methoxyacetamide (3c).** This compound was prepared in the same manner as compound **3a**, described above, and was purified by silica gel chromatography (eluent 3% MeOH in CH_2Cl_2) to yield pure **3c** with 64% yield. Mp = 159−163°C; MS (*m*/*z*) 435.0 (MH)$^+$; ^{1}H NMR (DMSO-d_6) δ 10.06 (s, 1H), 9.83 (s, 1H), 8.697 (d, J = 3 Hz, 1H), 8.571 (s, 1H), 8.277 (dd, J_1 = 5.7 Hz, J_2 = 2.7 Hz, 1H), 7.991 (dd, J_1 = 16.8 Hz, J_2 = 3.3 Hz, 1H), 7.909 (dd, J_1 = 16.5 Hz, J_2 = 0.9 Hz, 1H), 7.781 (d, J = 16.8 Hz, 1H), 7.46 (d, J = 16.5 Hz, 1H), 7.183 (t, J = 14.43 Hz, 1H), 4.09 (s, 1H), 3.43 (s, 3H). Anal. ($C_{17}H_{15}IN_4O_2$) C, H, N. HPLC conditions: C18 analytical column, 55% acetate buffer, pH = 3.8/45% acetonitrile, flow = 1 mL/min, R_t = 10.7 min.

***N*-{4-[(3,4-Dichloro-6-fluoro-phenyl)amino]-quinazoline-6-yl}-2-chloroacetamide (4a).** To a stirred solution of 6-amino-4-(3,4-dichloro-6-fluoro-phenylamino)quinazoline, **2a** (102 mg, 0.315 mmol), in dry THF under nitrogen at 0 °C, *N*,*N*-diisopropylethylamine (134 μL, 0.774 mmol) was added, followed by addition of chloroacetyl chloride (62 μL, 0.774 mmol). The mixture was stirred at 0 °C for 30 min, poured into saturated $NaHCO_3$, and extracted with EtOAc. The organic solution was dried with Na_2SO_4 and evaporated. The crude material was purified by silica gel chromatography (eluent 3% MeOH in CH_2Cl_2) to yield pure **4a** with 74% yield. Mp > 300 °C; MS (*m*/*z*) 399.0 (MH)$^+$; ^{1}H NMR (DMSO-d_6) δ 10.67 (s, 1H), 10.0 (s, 1H), 8.73 (s, 1H), 8.47 (s, 1H), 7.81 (m, 4H), 4.34 (s, 2H). Anal. ($C_{16}H_{10}Cl_3FN_4O$) C, H, N. HPLC conditions: C18 analytical column, 55% acetate buffer, pH = 3.8/45% acetonitrile, flow = 1 mL/min, R_t = 13.1 min.

***N*-{4-[(3-Bromo-phenyl)amino]-quinazoline-6-yl}-2-chloroacetamide (4b).** This compound was prepared in the same manner as compound **4a**, described above, and was purified by silica gel chromatography (eluent 3% MeOH in CH_2Cl_2) to yield pure **4b** with 40% yield. Mp = 300 °C; MS (*m*/*z*) 393 (100%, (MH$_2$)$^+$), 391 (99%, (MH)$^+$); ^{1}H NMR (DMSO-d_6) δ 10.63 (s, 1H), 9.98 (s, 1H), 8.71 (s, 1H), 8.58 (s, 1H), 8.14 (bs, 1H), 7.81 (m, 2H), 7.31 (m, 3H), 4.34 (s, 2H). Anal. ($C_{16}H_{12}BrClN_4O$) C, H, N. HPLC conditions: C18 analytical column, 55% acetate buffer, pH = 3.8/45% acetonitrile, flow = 1 mL/min, R_t = 13.1 min.

***N*-{4-[(3-Iodophenyl)amino]-quinazoline-6-yl}-2-chloroacetamide (4c).** This compound was prepared in the same manner as compound **4a**, described above, and was purified by silica gel chromatography (eluent 3% MeOH in CH_2Cl_2) to yield pure **4c** with 27% yield. Mp > 300 °C; MS (*m*/*z*) 439.0 (MH)$^+$; ^{1}H NMR (DMSO-d_6) δ 10.6 (s, 1H), 9.9 (s, 1H), 8.71 (s, 1H), 8.57 (s, 1H), 8.25 (m, 1H), 7.82 (m, 2H), 7.45 (d, J = 7.8 Hz, 1H), 7.19 (m, 2H), 4.34 (s, 2H). Anal. ($C_{16}H_{12}IClN_4O$) C, H, N. HPLC conditions: C18 analytical column, 55% acetate buffer, pH = 3.8/45% acetonitrile, flow = 1 mL/min, R_t = 13.1 min.

4-[(3,4-Dichloro-6-fluoro-phenyl)amino]-7-fluoro-6-nitroquinazoline (6a). 4-Chloro-7-fluoro-6-nitro-quinazoline[20] (0.245 g, 1.076 mmol) was dissolved in dichloromethane (7 mL), and 4,5-dichloro-2-fluoro-phenylamine (0.213 g, 1.18 mmol) dissolved in 2-propanol (14 mL) was added dropwise. The reaction mixture was stirred at room temperature for 30 min, while precipitation occurred. The precipitation was completed by the addition of hexane (25 mL); the crystals were filtered, dissolved with methanol, and neutralized with triethylamine. The orange solution was diluted with water to yield a yellow precipitate, which was filtered and washed with water. The yellow crystals were extracted with ethyl acetate and washed three times with $NaHCO_3$ solution (4%). The organic phase was dried over sodium sulfate, filtered, and evaporated under reduced pressure to yield pure **6a** with 30% yield. Mp = 232−235° C; MS (*m*/*z*) 371.0 (MH)$^+$; ^{1}H NMR (DMSO-d_6) δ 10.65 (bs, 1H), 9.48 (bs, 1H), 8.63 (s, 1H), 7.84 (m, 3H). HPLC conditions: C-18 column, 45% acetate buffer pH = 3.8/55% acetonitrile, flow = 1 mL/min, R_t = 11.03 min.

4-[(3-Bromophenyl)amino]-7-fluoro-6-nitroquinazoline (6b). This compound was prepared following a known procedure.[21] Mp = 198−201 °C; MS (*m*/*z*) 363.0 (M + H)$^+$; ^{1}H NMR (DMSO-d_6) δ 10.48 (s, 1H), 9.61 (d, J = 7.8 Hz, 1H), 8.75 (s, 1H), 8.15 (s, 1H), 7.8 (m, 2H), 7.38 (m, 2H). HPLC conditions: C-18 column, 60% acetate buffer, pH = 3.8/40% acetonitrile, flow = 1 mL/min, R_t = 24.48 min.

4-[(3,4-Dichloro-6-fluoro-phenyl)amino]-7-methylpiperazine-6-nitroquinazoline (7a). Compound **6a** (0.193 g, 0.52 mmol) was dissolved in dry THF (48 mL), and methylpiperazine (2.08 mmol, 230 μL) was added. The reaction mixture was refluxed for 20 h. THF was evaporated under reduced pressure; the residue was extracted with ethyl acetate and washed three times with a $NaHCO_3$ solution (4%). The organic phase was dried over Na_2SO_4, filtered, and evaporated, yielding pure **7a** with 91% yield. Mp = 196−199 °C; MS (*m/z*) 453.0 $(MH)^+$; ^{1}H NMR (DMSO-d_6) δ 8.95 (s, 1H), 8.4 (s, 1H), 7.85 (d, J = 7.5 Hz, 1H), 7.75 (d, J = 9.9 Hz, 1H), 7.22 (s, 1H), 3.06 (m, 4H), 2.43 (m, 4H), 2.22 (s, 3H). HPLC conditions: C-18 column, 45% acetate buffer, pH = 3.8/55% acetonitrile, flow =1 mL/min, R_t = 11 min.

4-(3-Bromophenylamino)-7-methlypiperazine-6-nitroquinazoline (7b). This compound was prepared in the same manner as compound **7a**, described above, to yield pure **7b** with 94% yield. Mp = 219−222 °C; MS (*m/z*) 445.0 $(MH)^+$; ^{1}H NMR (DMSO-d_6) δ 8.75 (s, 1H), 8.37 (s, 1H), 8.08 (m, 1H), 7.6 (m, 1H), 7.4 (s, 1H), 7.3 (m, 2H), 3.2 (t, J = 4.8 Hz, 4H), 2.6 (t, J = 4.8 Hz, 4H), 2.38 (s, 3H). HPLC conditions: C-18 column, 60% acetate buffer, pH = 3.8/40% acetonitrile, flow = 1 mL/min, R_t = 16.53 min.

4-(3,4-Dichloro-6-fluoro-phenylamino)-7-methylpiperazine-6-aminoquinazoline (8a). Compound **7a** (0.212 g, 0.469 mmol) was dissolved in 9:1 ethanol/water (62 mL) at room temperature, and after the solution was heated to 60 °C, hydrazine monohydrate (0.187 mmol, 91μL) and Ra−Ni (400 μL) were added. The reaction mixture was heated to 80 °C for 25 min. The brown-orange solution was cooled and filtered over cellite; the filtrate was evaporated under reduced pressure and dried to give pure **8a** with 91% yield. Mp = 221−225 °C; MS (*m/z*) 421.1 $(MH)^+$; ^{1}H NMR (DMSO-d_6) δ 9.28 (s, 1H), 8.26 (s, 1H), 7.97 (d, J = 7.8 Hz, 1H), 7.75 (d, J = 10.2 Hz, 1H), 7.32 (s, 1H), 7.17 (s, 1H), 5.21 (bs, 2H), 2.97 (bs, 4H), 2.54 (bs, 4H), 2.24 (s, 3H). HPLC conditions: C-18 column, 60% acetate buffer, pH = 3.8/40% acetonitrile, flow = 1 mL/min, R_t = 11.48 min.

4-(3-Bromophenylamino)-7-methlypiperazine-6-aminoquinazoline (8b). This compound was prepared in the same manner as compound **8a**, described above, and was purified by silica gel chromatography (eluent 5% MeOH in CH_2Cl_2) to yield pure **8b** with 55% yield. Mp = 93−95 °C; MS (*m/z*) 415.1 $(MH)^+$; ^{1}H NMR (DMSO-d_6) δ 9.39 (s, 1H), 8.37 (s, 1H), 8.22 (m, 1H, m), 7.84 (m, 1H), 7.47 (1H), 7.23 (2H), 7.15 (m, 1H), 5.13 (m, 2H), 2.97 (bs, 4H), 2.55 (bs, 4H), 2.24 (s, 3H). HPLC conditions: C-18 column, 60% acetate buffer, pH = 3.8/40% acetonitrile, flow = 1 mL/min, R_t = 7.5 min.

6-Acrylamido-7-methylpiperazine-4-[(3,4-dichloro-6-fluoro-phenyl)amino]-quinazoline (9a). Compound **8a** (0.08 g, 0.19 mmol) was dissolved in dry THF (15 mL) and stirred in an ice bath for 20 min. Diisopropylethylamine (0.132 mL, 0.76 mmol) was added; after 5 min, acryloyl chloride (0.031 mL, 0.38 mmol) was added, and the mixture was stirred for another 5 min at 0−5 °C. The reaction mixture was left to stir at room temperature for an additional 1 h under inert conditions. THF was evaporated; the residue was extracted with ethyl acetate and washed three times with a $NaHCO_3$ solution (4%). The organic phase was dried over Na_2SO_4, filtered, and evaporated. The crude material was purified by silica gel chromatography (eluent 5% MeOH in CH_2Cl_2) to give pure **9a** with 44% yield. Mp = 160−163 °C; MS (*m/z*) 475.0 $(MH)^+$; ^{1}H NMR (DMSO-d_6) δ 9.47 (s, 1H), 8.66 (s, 1H), 8.37 (bs, 1H), 7.79 (m, 2H), 7.28 (s, 1H), 6.68 (m, 1H), 6.3 (d, J = 16.8 Hz, 1H), 5.8 (d, J = 9.9 Hz, 1H), 2.98 (bs, 4H), 2.55 (bs, 4H), 2.24 (s, 3H). Anal. ($C_{22}H_{21}Cl_2FN_6O$·MeOH) C, H, N. HPLC conditions: C-18 column, 60% acetate buffer, pH = 3.8/40% acetonitrile, flow = 1 mL/min, R_t = 15.75 min.

6-Acrylamido-7-methylpiperazine-4-[(3-bromophenyl)-amino]- quinazoline (9b). This compound was prepared in the same manner as compound **9a**, described above, and purified by silica gel chromatography (eluent 5% MeOH in CH_2Cl_2) to yield pure **9b** with 62% yield. Mp = 125−127 °C. MS (*m/z*) 469 $(MH)^+$; ^{1}H NMR (DMSO-d_6) δ 9.79 (s, 1H), 9.54 (s, 1H), 8.69 (s, 1H), 8.54 (bs, 1H), 8.16 (bs, 1H), 7.87 (d, J = 8.1 Hz, 1H), 7.29 (m, 3H), 6.65 (m, 1H), 6.31 (d, J = 16.8 Hz, 1H), 5.8 (d, J = 9.9 Hz, 1H), 2.98 (bs, 4H), 2.54 (bs, 4H), 2.24 (s, 3H). Anal. ($C_{22}H_{23}BrN_6O$·2MeOH) C, H, N. HPLC conditions: C-18 column, 60% acetate buffer, pH = 3.8/40% acetonitrile, flow = 1 mL/min, R_t = 11.98 min.

Radiochemistry. Radiolabeling of Compound 5a. The radiosynthesis of the carbon-11-labeled compound **5a** was previously described.[14] Briefly, [^{11}C]-MeI was prepared according to a well-documented procedure and reacted with 8 mg of 4-monomethyl-amino-but-2-enoic acid [4-(3,4-dichloro-6-fluoro-phenylamino)-quinazolin-6-yl]-amide precursor in a mixture of 0.3 mL of anhydrous THF, 0.1 mL of CH_3CN, and 0.2 mL of DMSO at −20 °C. At the end of the 2-min distillation step, an average of 550 mCi (n = 30) was trapped in the reactor. The reactor was sealed and heated to 100 °C for 5 min. At the end of the 5-min reaction, THF and CH_3CN were removed under a flow of argon at 80 °C. The mixture was cooled to 40 °C, 0.6 mL of HPLC solvent (2% THF/60% CH_3CN/38% 0.1 M ammonium formate) was added, and the crude product [average of 370 mCi (n = 30)] was automatically injected to the HPLC [Bischoff Nucleosil 100-7-C18 reverse phase preparative column (7 μm, 250 mm × 16 mm), flow rate of 13 mL/min]. The labeled product was collected (R_t = 18 min) in a flask containing 60 μL of 1 M NaOH in 85 mL of water. The solution was passed through a C-18 cartridge (Waters Sep-Pak Plus, preactivated with 10 mL EtOH and 20 mL of sterile water), and the cartridge was washed with 4 mL of sterile water. The product was eluted with 0.75 mL of EtOH, followed by 4.25 mL of saline, and collected into the product vial after a total radiosynthesis time of 50 min. Identification of the product and chemical and radiochemical purities were determined by reversed phase HPLC C18 analytical column. The average (n = 30) final dose was approximately 0.74 GBq (20 mCi, 10% decay-corrected radiochemical yield); specific activity was 2.1−3.3 Ci/μmol.

C-11 radiolabeling of ML03 was described earlier.[20]

Biology. Production of A431 Cell Lysates as an EGFR Source. A431 human epidermoid vulval carcinoma cells, which overexpress the EGFR, were used for the production of active EGFR-containing membranes, as previously described.[26]

Cell-Free Assay. An evaluation of the EGFR autophosphorylation IC_{50} values was obtained by means of an ELISA screen, performed as depicted earlier.[26] For each compound, at least three independent assays that gave similar results were considered. Each assay was carried out using duplicate samples.

Cellular Assays. Irreversibility Test Protocol. The inhibitory potency of the different compounds, as well as the extent of irreversible EGFR inhibition, was evaluated in intact A431 cells, as already published.[26] For each compound, at least two different assays with similar results were considered. Each experiment was performed in duplicate.

Selective-Inhibition Assay. CSH12, DHER14, and NIH-PDGFR cells, expressing either the HER1−HER2 chimera, EGFR, or PDGFR, respectively, were used for the determination of inhibitory selectivity.[22−24] Cells (7.5×10^4) were grown in 6-well plates (35 mm diameter, Nalge Nunc) for 24 h and then incubated in 0.25% FCS-containing medium for an additional 24 h to ~90% confluence. Duplicate sets of cells were treated with the tested compounds at varying concentrations for 1 h. The final concentration of the vehicle in the medium was 0.05% DMSO, 0.1% EtOH. After removal of the inhibitor from the medium, PBS wash (×2), and addition of 0.25% serum-containing medium to the wells, the cells were stimulated with either 20 ng/mL human EGF for 5 min (CSH12 and DHER14 cells) or 50 ng/mL human $PDGF_{\beta\beta}$ for 10 min (NIHPDGFR cells) at 37°C. Following the stimulation with the growth factor, the cells were washed with cold PBS. Cell extracts were made by adding 0.4 mL of boiling Laemmli buffer (10% glycerol, 2% sodium dodecyl sulfate, 5% β-mercaptoethanol, 62.5 mM Tris·HCl, pH 6.8) containing 0.001% bromophenol blue to the cells, scraping them with a rubber policeman and heating to 100 °C for 10 min. For each

compound, at least two different assays with similar results were performed. Each experiment was carried out in duplicate.

Western Blot Analysis. Ten micrograms of protein lysates were separated by SDS−PAGE (8% polyacrylamide) and electrophoretically transferred to a nitrocellulose membrane. The membrane was blocked in TBST buffer (10 mM Tris-HCl, pH 7.4 (TBS), 0.2% Tween 20, 170 mM NaCl) containing 5% low-fat milk for 30 min, then probed overnight with the appropriate primary antibody. The membrane was washed thoroughly with TBST and incubated for 1 h with a horseradish peroxidase-conjugated anti-mouse IgG. Finally, the membrane was washed in TBST (4 × 5 min), and immunoreactive proteins were visualized using an enhanced chemiluminescence (ECL) detection reagent.

Blood Stability Assay. Blood samples were divided into 1 mL aliquots inside glass vials and incubated for 15 min at 37 °C under gentle shaking. A total of 100−150 μCi (25−50 μL) of [^{11}C]-**5a** solution (SA 150−220 μCi/nmol) was added to the blood samples for predetermined time periods, after which 1.5 mL of EtOH/THF (1:1) was added, and the blood samples were vortexed and centrifuged (5 min, 3000 rpm) for extraction of radioactive material. The entire vials were placed in a γ-counter (1480 Wizard 3") for measurement of total radioactivity; then the upper organic phase of the samples was loaded on TLC plates (Partisil LKC$_{18}$F silica gel, 5 × 20 cm, 250 μm layer thickness, Whatman), and the vials containing the nonextractable phase were placed once more in the γ-counter for measurement of the nonextractable radioactivity. The total extracted radioactivity was calculated by subtracting the nonextractable radioactivity from the total one. TLC plates were run for 50 min with 5% THF, 5% ammonium formate (0.1 M), 90% EtOH as a mobile phase and exposed for 1 h to phosphor imager plates (BAS-IP MS 2040 Fuji Photo Film Co., LTD) for visualization of radioactive bands. The plates were scanned with a BAS reader 3.1 version scanner and analyzed with TINA 2.10 g software.

Metabolite Study. Nude Hsd:RH-rnu/rnu male rats (200−300 g) were injected i.v. with [^{11}C]-**5a** (specific activity range of 200−500 μCi/μmol at time of injection, average volume of 211 ± 59 μL, and activity range of 130−550 μCi) and sacrificed at predetermined time points. Blood (1.5 mL) was drawn from the heart using a heparinized syringe and immediately mixed with 7.5 mL of 10% THF/ether for extraction of radioactivity. The liver (∼2 g) was excised, minced, and homogenized with 4 mL of saline in a tissue grinder (Fenbroek). The homogenate was mixed with 10 mL of 10% THF/ether for extraction of radioactive material. The total radioactivity of the samples was measured in a γ-counter and extracted as previously described,[19] and the nonextractable radioactivity was measured again in the γ-counter for further calculations. The organic extracted phase was loaded onto TLC plates with 5% THF, 10% NaCl (0.1 M) solution, 85% MeOH as mobile phase. As for the blood-stability assay, radioactive bands were visualized by a phosphor imager plate.

Acknowledgment. Support was provided by TK-Signal, Ltd., Jerusalem, Israel, and by Rotem Industries Ltd., Be'er Sheva, Israel.

Supporting Information Available: Elemental analysis of group A−D inhibitors of EGFR. This material is available free of charge via the Internet at http://pubs.acs.org.

References

(1) Levitzki, A.; Gazit, A. Tyrosine kinase inhibition: an approach to drug development. *Science* **1995**, *267*, 1782−1788.
(2) Yarden, Y.; Schlessinger, J. Self-phosphorylation of epidermal growth factor receptor: evidence for a model of intermolecular allosteric activation. *Biochemistry* **1987**, *26*, 1434−1442.
(3) Cohen, S.; Ushiro, H.; Stoscheck, C.; Chinkers, M. A native 170,-000 epidermal growth factor receptor-kinase complex from shed plasma membrane vesicles. *J. Biol. Chem.* **1982**, *257*, 1523−1531.
(4) Iwashita, S.; Kobayashi, M. Signal transduction system for growth factor receptors associated with tyrosine kinase activity: epidermal growth factor receptor signaling and its regulation. *Cell. Signalling* **1992**, *4*, 123−132.
(5) Voldborg, B. R.; Damstrup, L.; Spang-Thomsen, M.; Poulsen, H. S. Epidermal growth factor receptor (EGFR) and EGFR mutations, function and possible role in clinical trials. *Ann. Oncol.* **1997**, *8*, 1197−1206.
(6) Stoscheck, C. M.; Carpenter, G. Characterization of the metabolic turnover of epidermal growth factor receptor protein in A-431 cells. *J. Cell. Physiol.* **1984**, *120*, 296−302.
(7) Ritter, C. A.; Artega, C. L. The epidermal growth factor receptor-tyrosine kinase: a promising therapeutic target in solid tumors. *Semin. Oncol.* **2003**, *30*, 993−1011.
(8) Raymond, E.; Faivre, S.; Armand, J. P. Epidermal growth factor receptor tyrosine kinase as a target for anticancer therapy. *Drugs* **2000**, *60*, 15−23; discussion 41−42.
(9) Salomon, D. S.; Brandt, R.; Ciardiello, F.; Normanno, N. Epidermal growth factor-related peptides and their receptors in human malignancies. *Crit. Rev. Oncol. Hematol.* **1995**, *19*, 183−232.
(10) Cohen, M. H.; Williams G. A.; Sridhara, R.; Chen, G.; Pazdur, R. FDA drug approval summary: Gefitinib (ZD 1839) (Iressa) tablets. *The Oncologist* **2003**, *8*, 303−306.
(11) FDA News. http://www.fda.gov/bbs/topics/NEWS/2004/NEW01024.html.
(12) Mishani, E.; Bonasera, T. A.; Rozen, Y.; Ortu, G.; Gazit, A.; Levitzki, A. Fluorinated EGFR-TK inhibitors-based tracers for PET. *J. Labelled Compd. Radiopharm.* **1999**, *42*, S27−S29.
(13) Mishani, E.; Abourbeh, G.; Ortu, G.; Rozen, Y.; Ben-David, I.; Froimovaci, S.; Dissoki, S.; Gazit, A.; Levitzki, A. Novel EGFR irreversible tyrosine kinase inhibitor candidates for the diagnostic and therapeutic treatment of cancer, *J. Labelled Compd. Radiopharm.* **2003**, *46*, S115.
(14) Mishani, E.; Abourbeh, G.; Rozen, Y.; Laki, D.; Levitzki, A. Carbon-11 labeling of 4-(dimethylamino)-but-2-enoic acid [4-(phenylamino)-quinazoline-6-yl]-amides. A new class of EGFR irreversible inhibitors. *J. Labelled Compd. Radiopharm.* **2003**, *46*, S2.
(15) VanBrocklin, H. F.; Dorff, P. N.; Vasdev, N.; O'Neil, J. P.; Nandanan, E.; Gibbs, A. R. Synthesis of 2′-, 3′- and 4′-[F18]-fluoroanilinoquinazoline. *J. Labelled Compd. Radiopharm.* **2003**, *46*, S117.
(16) Ackermann, U.; Tochon-Danguy, H.; Nice, E.; Nerrie, M.; Young, K.; Sachinidis, J.; Scott, A. Synthesis, radiolabeling and biological evaluation of derivatives of the P210BCR-ABL tyrosine kinase inhibitor AG957, *J. Labelled Compd. Radiopharm.* **2003**, *46*, S118.
(17) Kesarios, N.; Tochon-Danguy, H.; Ackermann, U.; Sachinidis, J.; Lambert, J.; Nerrie, M.; Nice, E.; Scott, A. Synthesis and radiolabeling of a tyrosine kinase inhibitor of erbB2/neu (HER2) receptors. *J. Labelled Compd. Radiopharm.* **2003**, *46*, S119.
(18) Bonasera, T. A.; Ortu, G.; Rozen, Y.; Krais, R.; Freedman, N. M.; Chisin, R.; Gazit, A.; Levitzki, A.; Mishani, E. Potential (18)F-labeled biomarkers for epidermal growth factor receptor tyrosine kinase. *Nucl. Med. Biol.* **2001**, *28*, 359−374.
(19) Ortu, G.; Ben-David, I.; Rozen, Y.; Freedman, N. M. T.; Chisin, R.; Levitzki, A.; Mishani, E. Labeled EGFRTK irreversible inhibitor (ML03). In vitro and in vivo properties, potential as PET biomarker for cancer and feasibility as anticancer drug. *Int. J. Cancer* **2002**, *101* (4), 360−370.
(20) Ben-David, I.; Rozen, Y.; Ortu, G.; Mishani, E. Radiosynthesis of ML03, a novel positron emission tomography biomarker for targeting epidermal growth factor receptor via the labeling synthon: [C-11]Acryloyl chloride, *Appl. Radiat. Isot.* **2003**, *58*, 209−217.
(21) Fry, D. W.; Bridges, A. J.; Denny, W. A.; Doherty, A.; Greis, K. D.; Hicks, J. L.; Hook, K. E.; Keller, P. R.; Leopold, W. R.; Loo, J. A.; McNamara, D. J.; Nelson, J. M.; Sherwood, V.; Smaill, J. B.; Trumpp-Kallmeyer, S.; Dobrusin, E. M. Specific, irreversible inactivation of the epidermal growth factor receptor and erbB2, by a new class of tyrosine kinase inhibitor. *Proc. Natl. Acad. Sci. U.S.A.* **1998**, *95*, 12022−12027.
(22) Lee, J.; Dull, T. J.; Lax, I.; Schlessinger, J.; Ullrich, A. HER2 cytoplasmic domain generates normal mitogenic and transforming signals in a chimeric receptor. *EMBO J.* **1989**, *8*, 167−73.
(23) Honegger, A.; Dull, T. J.; Szapary, D.; Komoriya, A.; Kris, R.; Ullrich, A.; Schlessinger, J. Kinetic parameters of the protein tyrosine kinase activity of EGF-receptor mutants with individually altered autophosphorylation sites. *EMBO J.* **1988**, *7*, 3053−3060.
(24) Shawver, L. K.; Schwartz, D. P.; Mann, E.; Chen, H.; Tsai, J.; Chu, L.; Taylorson, L.; Longhi, M.; Meredith, S.; Germain, L.; Jacobs, J. S.; Tang, C.; Ullrich, A.; Berens, M. E.; Hersh, E.; McMahon, G.; Hirth, K. P.; Powell, T. J. Inhibition of platelet-derived growth factor-mediated signal transduction and tumor growth by N-[4-(trifluoromethyl)-phenyl]5-methylisoxazole-4-carboxamide. *Clin. Cancer Res.* **1997**, *3* (7), 1167−77.
(25) Tsou, H. R.; Mamuya, N.; Johnson, B. D.; Reich, M. F.; Gruber, B. C.; Ye, F.; Nilakantan, R.; Shen, R.; Discafani, C.; DeBlanc, R.; Davis, R.; Koehn, F. E.; Greenberger, L. M.; Wang, Y. F.; Wissner, A. 6-Substituted-4-(3-bromophenylamino)quinazolines

as putative irreversible inhibitors of the epidermal growth factor receptor (EGFR) and human epidermal growth factor receptor (HER-2) tyrosine kinases with enhanced antitumor activity. *J. Med. Chem*. **2001**, *44*, 2719−2734.

(26) Smaill, J. B.; Palmer, B. D.; Rewcastle, G. W.; Denny, W. A.; McNamara, D. J.; Dobrusin, E. M.; Bridges, A. J.; Zhou, H.; Showalter, H. D.; Winters, R. T.; Leopold, W. R.; Fry, D. W.; Nelson, J. M.; Slintak, V.; Elliot, W. L.; Roberts, B. J.; Vincent, P. W.; Patmore, S. J. Tyrosine kinase inhibitors. 15. 4-(Phenylamino)quinazoline and 4-(phenylamino)pyrido[d]pyrimidine acrylamides as irreversible inhibitors of the ATP binding site of the epidermal growth factor receptor. *J. Med. Chem*. **1999**, *42*, 1803−1815.

(27) Mishani, E.; Abourbeh, G.; Rozen, Y.; Jacobson, O.; Laky, D.; Ben David, I.; Levitzki, A.; Shaul, M. Novel carbon-11 labeled 4-(dimethylamino)-but-2-enoic acid [4-(phenylamino)-quinazoline-6-yl]-amides: potential PET bioprobes for molecular imaging of EGFR-positive tumors. *Nucl. Med. Biol*. **2004**, *31*, 469−476.

(28) Rewcastle, G. W.; Palmer, B. D.; Bridges, A. J.; Showalter, H. D.; Sun, L.; Nelson, J.; McMichael, A.; Kraker, A. J.; Fry, D. W.; Denny, W. A. Tyrosine kinase inhibitors. 9. Synthesis and evaluation of fused tricyclic quinazoline analogues as ATP site inhibitors of the tyrosine kinase activity of the epidermal growth factor receptor. *J. Med. Chem*. **1996**, *39*, 918−928.

JM0580196